12-2010

The Effect of Bonner Sphere Borehole Orientation on Neutron Detector Response

John Macdougall Brittingham
University of Tennessee - Knoxville, jbritti1@utk.edu

To the Graduate Council:

I am submitting herewith a thesis written by John Macdougall Brittingham entitled "The Effect of Bonner Sphere Borehole Orientation on Neutron Detector Response." I have examined the final electronic copy of this thesis for form and content and recommend that it be accepted in partial fulfillment of the requirements for the degree of Master of Science, with a major in Nuclear Engineering.

Lawrence H. Heilbronn, Major Professor

We have read this thesis and recommend its acceptance:

Ronald E. Pevey, Martin L. Grossbeck

Accepted for the Council:
Carolyn R. Hodges

Vice Provost and Dean of the Graduate School

(Original signatures are on file with official student records.)

To the Graduate Council:

I am submitting herewith a thesis written by John Macdougall Brittingham entitled The Effect of Bonner Sphere Borehole Orientation on Neutron Detector Response. I have examined the final electronic copy of this thesis for form and content and recommend that it be accepted in partial fulfillment of the requirements for the degree of Master of Science, with a major in Nuclear Engineering.

<u>Lawrence H. Heilbronn</u> , Major Professor

We have read this thesis and recommend its acceptance:

<u>Ronald E. Pevey</u>

<u>Martin L. Grossbeck</u>

Accepted for the Council:

<u>Carolyn R. Hodges</u>
Vice Provost and Dean of the Graduate School

(Original signatures are on file with official student records.)

The Effect of Bonner Sphere Borehole Orientation on Neutron Detector Response

A Thesis
Presented for the
Master of Science
Degree
The University of Tennessee, Knoxville

John Macdougall Brittingham
December 2010

Copyright

Dedication

For Deseree and Marin

Acknowledgments

I would like to thank my advisor, Professor Lawrence Heilbronn, for his support and advice both concerning this thesis and my continuing education as a nuclear engineer. I would also like to thank Professors Martin Grossbeck and Ronald Pevey, both for serving on my thesis committee and for their instruction and guidance. Finally, I wish to thank the Department of Nuclear Engineering at the University of Tennessee-Knoxville. I have truly enjoyed every moment of my ongoing education.

Abstract

This thesis investigates the differences in Bonner Sphere detector response for anisotropic neutron fields as a function of borehole orientation. Monte Carlo simulations using MCNPX were used to calculate the difference in detector response between Bonner Spheres with a borehole oriented directly behind a unidirectional neutron field and Bonner Spheres in which the borehole is normal to the neutron flux. The differences in detector response depend on the size of the Bonner Sphere and the energy of the incident flux and are likely due to the Bonner Sphere's geometry. These effects could introduce significant error in the determination of the neutron field's energy spectrum for an anisotropic neutron flux.

Table of Contents

List of Tables

List of Figures

The Effect of Bonner Sphere Borehole Orientation on Neutron Detector Response

Introduction

Function of Bonner Spheres

Bonner Spheres provide a convenient and accessible method to measure the neutron energy spectrum with a scintillation detector and several moderating spheres of varying diameters. All spheres are exposed to the same neutron flux.[1] As Figure 1 illustrates, the polyethylene moderates the neutrons that pass through it, making interaction inside the detector material more likely. The setup used in this study employed a Lithium-glass scintillation detector. Scintillation detectors, such as ^{3}He, BF_3, and Li-glass detectors are particularly sensitive to thermal neutrons. Therefore, the increased moderation of a larger polyethylene sphere increases the detector response for higher energy neutrons. As the sphere's diameter increases, the number of neutrons with lower initial energy that reach the detector decreases, giving each sphere a unique response function to the incoming neutron energy. Figure 2 demonstrates this effect. A sphere of larger diameter will increase the incident neutron energy at which the response function will peak; therefore, evaluating the response of a detector in Bonner Spheres of varying width enables the experimenter to determine the energy spectrum of the incident neutrons, which would otherwise be impossible with a scintillation detector alone.

---

[1] Glenn F. Knoll, *Radiation Detection and Measurement* (3rd ed), John Wiley & Sons, Inc. (2000), p. 539-40.
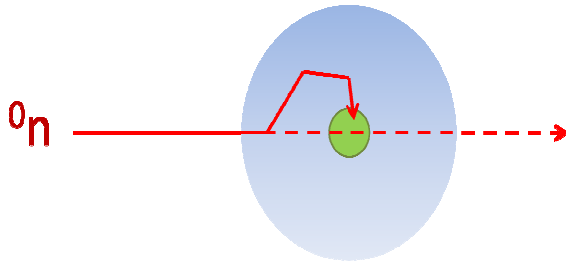
Figure 1: Bonner Spheres moderate neutrons, increasing the probability of a detection event.[2]
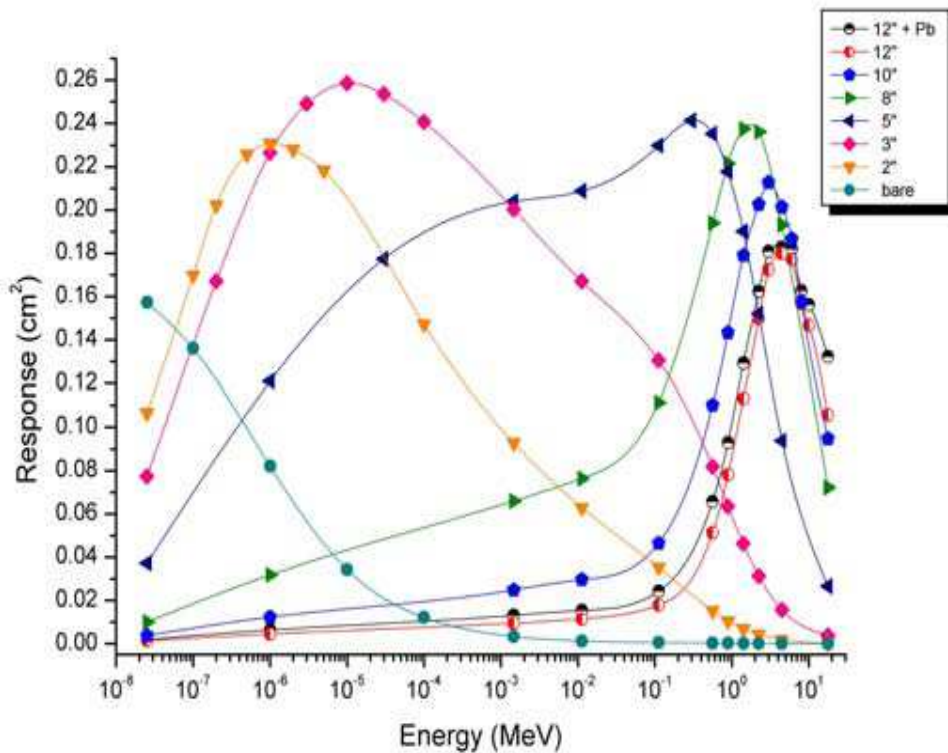
Figure 2: Example of Bonner Sphere Response Functions for varying diameters.[3]

To achieve this result, the experimenter will ascertain the detector response for the same neutron source field for each available diameter sphere and use an unfolding code. Unfolding codes work by examining the detector's varied responses to different energy spectra given the

---

[2] Adapted from Knoll, p. 539.

[3] J.A. Cruzate, J.L. Carelli, & B.N. Gregory, Bonner Sphere Spectrometer, presented at Workshop on Uncertainty Assessment in Computational Dosimetry: A Comparison of Approaches, Bologna, Italy (8-10 October 2007).

diameter of the Bonner Sphere and produce an approximate spectrum based on a starting

spectrum input by the user. The code uses a multigroup approximation where the relevant

energies are divided into groups for ease of calculation. Detector group response R_i to a given

energy group which accounts for the spectrum from E_i to E_{i+1} can be expressed as:

$$R_i = \int_{E_i}^{E_{i+1}} \sigma(E)\varphi(E)dE \cong \frac{\int_{E_i}^{E_{i+1}} \sigma(E)\varphi(E)dE}{\int_{E_i}^{E_{i+1}} \varphi(E)dE} * \int_{E_i}^{E_{i+1}} \varphi(E)dE = \sigma_i \varphi_i \quad (1)$$

where $\varphi(E)$ is the scalar neutron flux, $\sigma(E)$ is the detector's sensitivity to neutrons of energy E, σ_i

is the sensitivity of the detector to neutrons in energy group i, and φ_i is the group flux. The

measured detector response R is therefore equal to the sum of the group response functions over

all groups:

$$R = \sum_i R_i = \sum_i \sigma_i \varphi_i \qquad (2)$$

Both the detector response to a given energy field (σ_i) and the detector response to the actual

energy field in question (R) are known; therefore, calculating the spectrum of the incident

neutron flux can be reduced to a set of simultaneous equations which can be used to approximate

the spectrum of the neutron flux using an algorithm such as BUMS, SPUNIT, MAXED, or

SAND-II.[4]

Detector Characteristics

        The detector placed in the Bonner Sphere for this experiment was a 2 mm diameter, 2

long cylindrical Lithium-glass detector. The material for the detector was modeled from

MCNPX's material library as a 1:1:2 ratio of Lithium, Silicon, and Oxygen. Li-glass detectors

---

[4] Jeremy Sweezy, Nolan Hertel, & Ken Veinot. BUMS—Bonner Sphere Unfolding Made Simple: an HTML based multisphere neutron spectrometer unfolding package. 476 *Nuclear Instruments and Methods in Physics Research A* 263-69 (2002).

are normally enriched in ^{6}Li, due to ^{6}Li's higher neutron absorption cross section. The detector

used in this simulation used Li that was 95% ^{6}Li and 5% ^{7}Li. The cylindrical axis of the detector

was oriented along the cylindrical axis of the bore hole in both the 0° and 90° cases.

Simulation Setup

Bonner Sphere Setup

The simulated experimental set up involved a series of Bonner Spheres placed

downstream of a cylindrical beam of neutrons. The Bonner Spheres were constructed entirely of

polyethelene (CH_2) with a 1 cm diameter detector borehole drilled to the center. The Bonner

Sphere diameters are 2", 3", 5", 8", 10", and 12". Data was also calculated with bare detectors in

each case for completeness. A schematic diagram of the experimental setup appears in Figure 3.
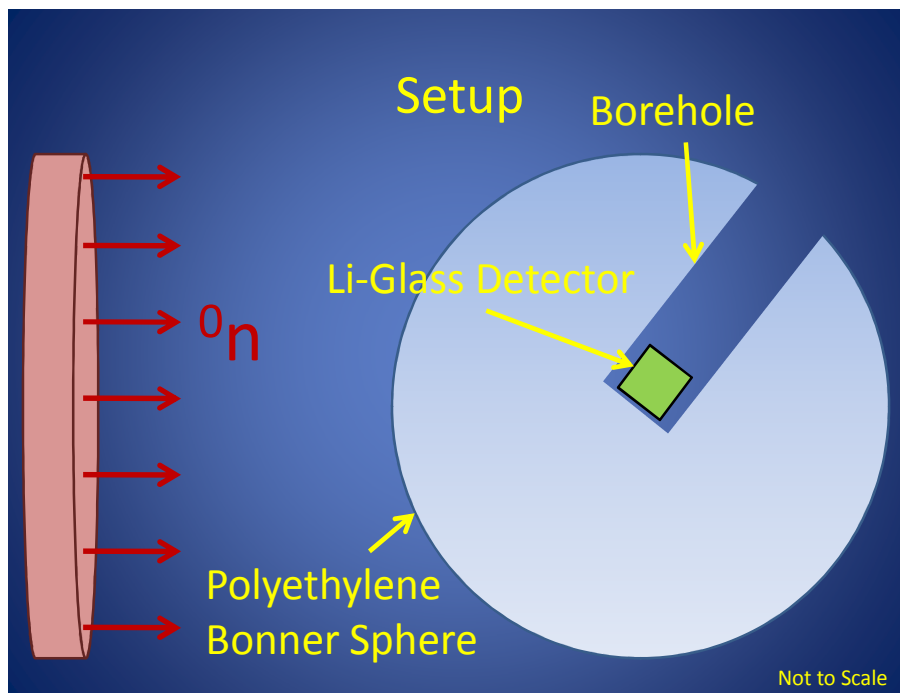
Figure 3: Simulated Experimental Setup – a cylindrical beam of neutrons strikes the Bonner sphere and Li-glass detector from the left. The diameter of the beam is the same as the diameter of the polyethylene sphere.
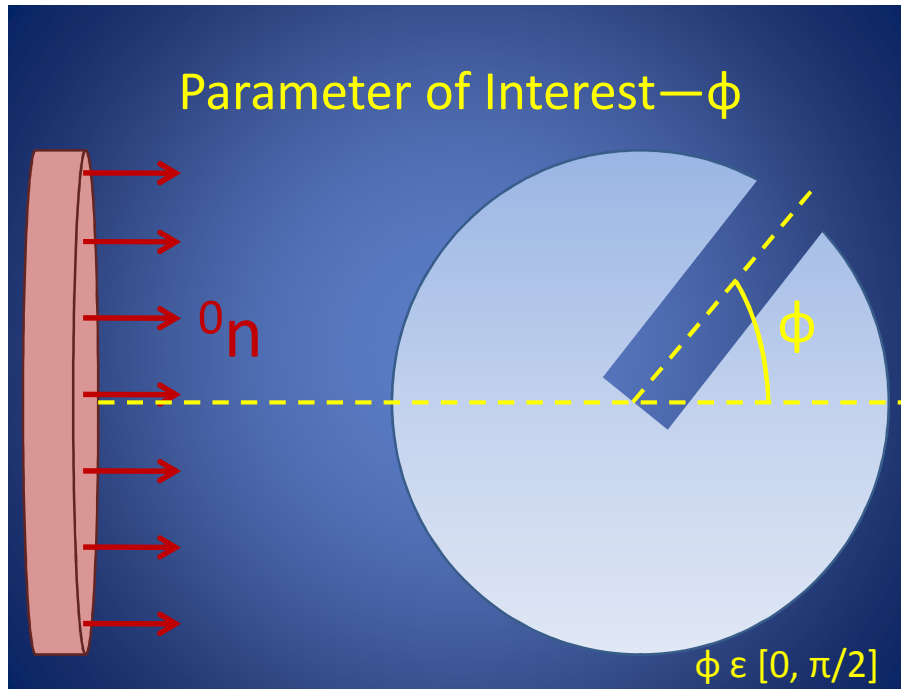
Figure 4: Borehole Angle

Simulations were conducted with the borehole oriented at 0° (borehole opposite the source) and 90° (borehole orthogonal to source) in all cases to determine the difference in detector response. For the 2" sphere, data between 0° and 90° was taken to more thoroughly examine the angular independence. Figure 4 illustrates the meaning of the borehole angle. Detector response for each case was compared by calculating the average flux inside the detector.

Source Production

The source for this problem consists of a uniform beam of neutrons with evenly distributed energy within one of thirty-one energy bins of interest. A table showing the limits of each energy bin appears below. The neutrons are produced on the surface of a disk with diameter equal to that of the Bonner Sphere. No neutrons were created outside of the Bonner Sphere diameter because those neutrons would entirely pass the apparatus without colliding and would exit the geometry uncollided, contributing nothing to the result. The neutron production is

then normalized to the cross sectional area of the Bonner Sphere to account for the differences in the beam strength incident on the Bonner Spheres.

Because a neutron is equally likely to be born at any point in the disk of radius R, the probability density function p(r) is proportional to the radius. Because the problem is symmetric, there is no dependence on polar angle θ.

$$p(r, \theta)dA = \frac{dA}{\pi R^2} = \frac{rdrd\theta}{\pi R^2} \qquad (3)$$

$$p(r)dr = \int_0^{2\pi} \frac{rdrd\theta}{\pi R^2} = \frac{2rdr}{R^2} \qquad (4)$$

$$p(r) = \frac{2r}{R^2} \propto r \qquad (5)$$

Therefore, the source distribution can be programmed into the Source Probability function as a linear function of radius. Although MCNPX uses a uniform source distribution as its default, the explicit inclusion of a uniform Source Probability function simplified the programming steps required to introduce a Source Bias function to reduce the variance of the detector response.

Table 1: Energy groups used for the experimental simulation.

Bin	Lower E (MeV)	Upper E (MeV)	Bin	Lower E (MeV)	Upper E (MeV)
1	1.00E-08	4.14E-07	17	2.48E-02	5.25E-02
2	4.14E-07	6.83E-07	18	5.25E-02	1.11E-01
3	6.83E-07	1.45E-06	19	1.11E-01	2.24E-01
4	1.45E-06	3.06E-06	20	2.24E-01	4.51E-01
5	3.06E-06	6.48E-06	21	4.51E-01	9.07E-01
6	6.48E-06	1.37E-05	22	9.07E-01	1.87E+00
7	1.37E-05	2.90E-05	23	1.87E+00	3.68E+00
8	2.90E-05	6.14E-05	24	3.68E+00	7.41E+00
9	6.14E-05	1.30E-04	25	7.41E+00	1.49E+01
10	1.30E-04	2.75E-04	26	1.49E+01	2.58E+01
11	2.75E-04	5.93E-04	27	2.58E+01	4.47E+01
12	5.93E-04	1.23E-03	28	4.47E+01	7.73E+01
13	1.23E-03	2.61E-03	29	7.73E+01	1.34E+02
14	2.61E-03	5.53E-03	30	1.34E+02	2.31E+02
15	5.53E-03	1.17E-02	31	2.31E+02	4.00E+02
16	1.17E-02	2.48E-02			

The experiment was conducted in 31 energy ranges for each sphere. These ranges are those that are normally used to conduct Bonner Sphere simulations and extend from 1×10^{-8} to 400 MeV, covering all energy ranges of interest for neutron radiation. Initial neutron energy was uniformly sampled within each group.

Coding the Simulation

Producing the Files

Running one complete set of Monte Carlo simulations required producing MCNPX input files for both the 0 and 90° orientation for 31 separate energy bins for 7 different Bonner sphere diameters, including the bare detector. Therefore, 434 separate simulations are required to produce one complete set of results. Manually programming and changing 434 separate files to obtain the best results was not a practical approach to this problem. Efficient production of these files required using the development capabilities of Microsoft Word and Excel as well as Visual Basic. First, the basic MCNPX input file was programmed using the MCNP Visual Editor. Then, the parameters that changed for each problem, such as the energy limits and sphere size were listed in a Microsoft Excel file. The MCNPX input file was then copied to a Microsoft Word file and was programmed as a Mail Merge, fed from the data from the Excel file. The Mail Merge function was then utilized to produce a single 434-page Word file with each page representing an individual MCNPX file. A Visual Basic Macro was then executed to copy each individual MCNPX program into its separate Word file, which was saved as a .txt file. A batch file was then used to run the individual MCNPX files sequentially and save them to individual output files. Upon completion of the MCNPX run, a separate Visual Basic Macro was used to copy the mean and variance of the appropriate tally back into a single Word file, which was then cut and pasted into Microsoft Excel for analysis.
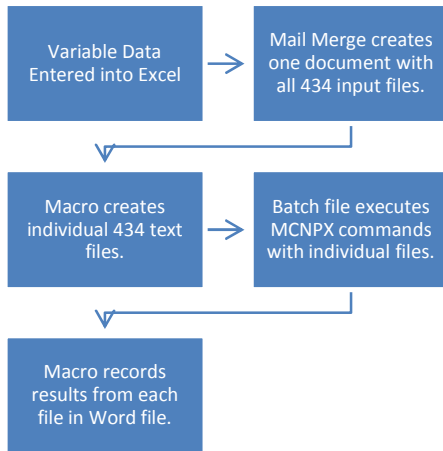
Figure 5: MCNPX File Creation Process

Variance Reduction Techniques

An analog Monte Carlo simulation without variance reduction controls will produce the desired end result, but limitations on computer time and random number generation make the process inefficient. The estimated relative error of the result of a Monte Carlo simulation is inversely proportional to the square root of the number of histories run:

$$R \propto \frac{1}{\sqrt{N}} \quad (6)$$

where N is the number of histories that the simulation has run.[5] The MCNPX Code can produce only 2^{46} (approximately 7×10^{13}) unique pseudorandom numbers.[6] The relative insensitivity of the simulation apparatus to segments of the energy spectra (especially above 100 MeV) made variance reduction strategies essential in this simulation to produce an answer with an acceptable variance. Running histories beyond the random number period will appear to reduce variance but will in fact contribute no additional useful information to the calculation of the mean.

---

[5] X-5 Monte Carlo Team, *MCNP--A General Monte Carlo N-particleTransport Code, Version 5* (Feb. 2008 ed.), Vol. 1, p. 6.

[6] D.B. Pelowitz, ed., *MCNPX User's Manual* (Feb. 2008 ed.), Table 5-116, p. 5-185.

Another limitation on the ability to produce results within acceptable error is the availability of time and processing resources to run long simulations. The computer resources used to complete this simulation required on average two hours to run 200 million histories for an analog Monte Carlo simulation, which equates to approximately thirty-six days to run all 434 simulations. Inclusion of splitting and other variance reduction techniques makes run-time potentially longer.

The most important variance reduction technique employed in this simulation was source biasing. Source biasing allows the user to implement a source distribution that is different from the natural source distribution in order to ensure that more histories reach the detector and contribute to the result.[7] This technique produces the same mean as the analog Monte Carlo process because a weight correction is applied to all particles such that the particles that are created more often than they naturally would be count for less at the detector. Conversely, particles that are created less frequently than they would be naturally would count for more at the detector. The natural source probability in this problem is a uniform field of neutrons emanating from a disk with diameter equal to that of the relevant Bonner Sphere. However, because the detector is located at the center of the sphere and has a diameter of only 2 mm, the neutrons that are created at the fringe of the disk are unlikely to reach the detector. The modified distribution creates bins such that half of the neutrons are born within a 2 cm radius of the center and the other half are created in the outer areas. As a result, more neutrons with less weight will create flux across the detector, leading to more detection events and less variance in the Lithium-glass detector.

This technique resulted in significantly less variance, especially in the Bonner Spheres with a larger diameter. As neutrons are created closer to the fringe of the Bonner Sphere, they

---

[7] X-5 Monte Carlo Team, Vol. 2, p. 155.

have shorter paths across the sphere in which to collide initially and then have a much longer path through the sphere to the detector. Overall, judicious use of source biasing will allow results with lower variance, which will require fewer histories and in turn less computer time.

Other variance reduction techniques that were considered included importance weighting, forced collisions inside the polyethylene portion of the Bonner Spheres, exponential transformation, and weight windows. Ultimately, none of these techniques were employed because source biasing was sufficient to produce results with acceptable variance. The sample run of one scenario using forced collisions within the Bonner Sphere took almost 23 hours to run 200 million histories with only a marginal improvement of the statistics. Importance weighting was not practical because it would have required programming the Bonner sphere as several concentric spherical shells, which would have been logistically difficult to program for 434 cases. Using weight windows would have achieved the same result without cell division and would have provided the capability to reduce importances on the rear side of the sphere; however, it was also logistically difficult to program for all 434 cases. Although it was not considered, approximating the detector with a point flux tally would have greatly simplified the calculations and led to low-variance results with a corresponding reduction in computing time. Ultimately, simply producing most particles near the center of the sphere where they were more likely to interact and enter the detector was capable of producing the same results as a lower cost of computer time.

Example of Input Code

       The following shows an example of the MCNPX code that was run in this simulation.[8]

This example shows the input for the lowest energy bin for the 2" Bonner Sphere.

```
c ====================Cell Cards=========================
   1   2   -2.5   -3   4   -6         $detector volume
   2   0            -7   -2   4   #1   $housing (vacuum)
   3   3   -2.2   -7   -4   5         $glass in borehole
   4   1   -0.92  -8 #1  #2  #3       $poly sphere
   5   0            8  -9  #3         $cosmos
   6   0            9                 $outside cosmos

c =============Surface Cards=================
   1      pz 20               $surface for source
   2   1  pz 0                $middle of sphere, edge of glass
   3   1  pz -0.02375         $edge of glass; front face of detector
   4   1  pz -0.2             $back face of detector
   5   1  pz -15.24           $end of borehole (accounts for all spheres)
   6   1  cz 0.1              $2 mm diameter detector
   7   1  cz 0.5              $borehole and can
   8      so 10.16001         $poly sphere
   9      so 500              $cosmos

c ================Control Cards=============
mode  n
c ====================Material Cards===========
m1    1001.50c   0.6667
      6000.50c   0.3333
m2    3006.50c   0.02162
      3007.50c   0.00114
      14000.50c  0.02276
      8016.50c   0.04552
m3    14000.50c  1
      8016.50c   2
tr1    0 0 0 1 0 0 0 1 0 0 0 1
imp:n  1   4r    0
nps    25000000
mt1   poly.01t                     $SAB treatment at 300K
c
c ========================Source Card=========================
sdef  erg=d1   par=1   sur=1   pos=0 0 20   rad=d2   dir=-1
```

---

[8] This input file was adapted from an MCNPX input file written to perform a simulation on the University of Tennessee nuclear engineering department's Bonner Spheres. The original file was produced by Professor Laurence Miller's team.

```
si1    7.408   14.92    401
sp1     0   1    0
si2     0.00001   1    2     10.16
sp2    -21    1
sb2     0   0.4    0.4    0.2
```
c ==========================Tally Card==========================
f4:n 1

Data and Analysis

Response of Bare Detector

As an initial manner, the difference between the bare detector response for the 0 and 90°

cases was analyzed. As Figures 6 and 7 illustrate, the 90° case resulted in a 90° detector response

that was approximately 0.59 times the response for the 0° case.

Any analysis of the effect of an anisotropic neutron field must begin with an analysis of

the difference in detector response for the bare detector. The cylindrical shape of the detector

will lead to a significant expected difference between neutrons entering parallel to and

perpendicular to the cylinder's z-axis. For the purposes of this analysis, it is assumed that the

neutron's first collision in the detector is the only significant source of detector response.

Furthermore, it is assumed that every neutron collision inside the detector causes a uniform

response in the detector, regardless of the energy loss. The 0° detector's response is

straightforward because the path length of each uncollided neutron through the detector will be

the height of the detector because its path through the detector is along the cylindrical axis (the z-

axis). The detector's response to neutrons entering perpendicular to the cylindrical axis (in the rθ

plane) is more complicated because each neutron's path length will differ based on its point of
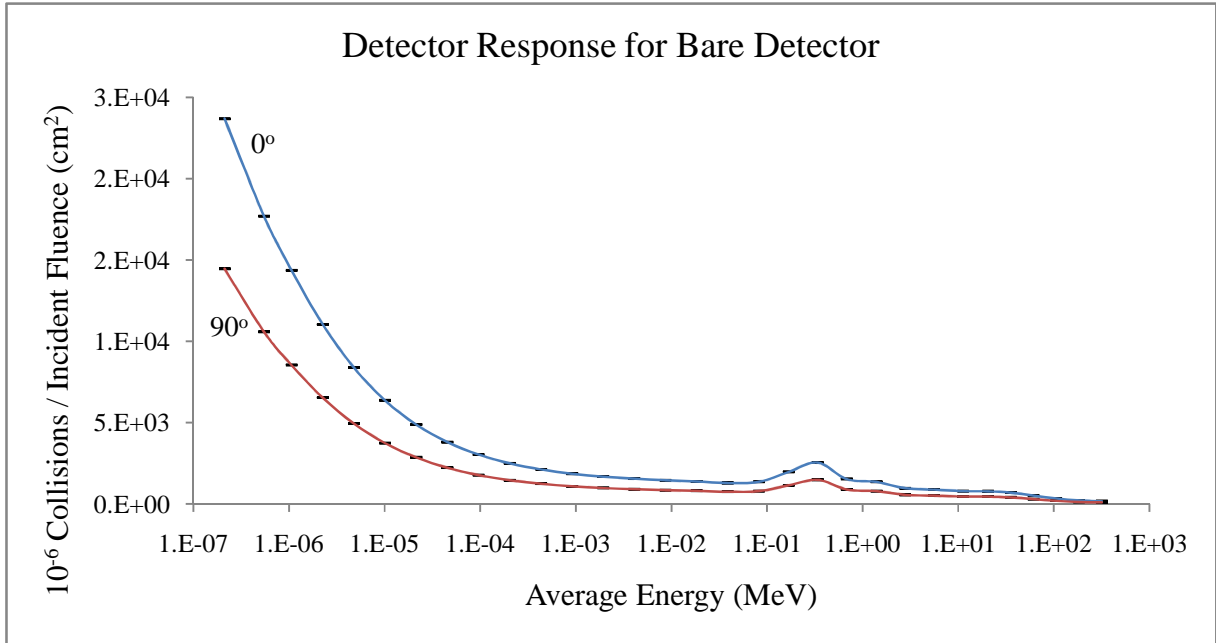
entry into the detector.
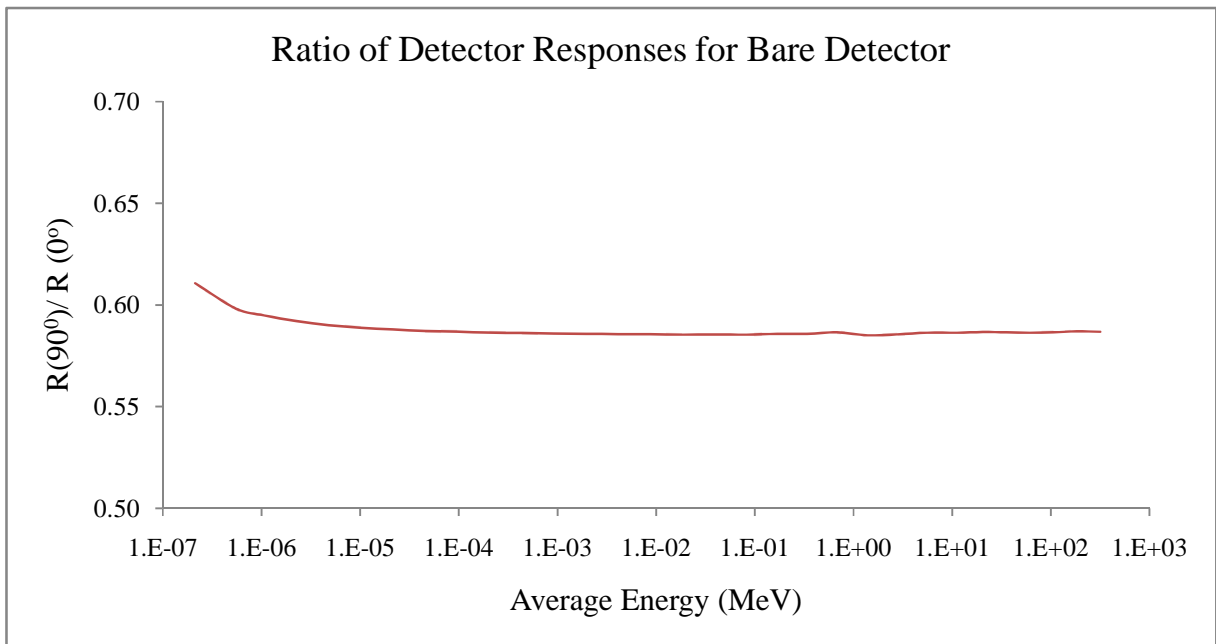
12

Figure 6: Bare Detector Response

Figure 7: Ratio of Detector Response Functions for Bare Detector

13

Beginning with the response at 0°, the expected detector response is:

$$R = \varphi_0(1 - e^{-\mu L}) \quad (7)$$

where φ_0 is the incident neutron flux, L is the length of the detector and μ is the macroscopic cross section of the detector material. It is further assumed that μL is small, so the exponential can be Taylor-expanded:

$$e^{-\mu L} = \sum_{n=0}^{\infty} \frac{(-\mu L)^n}{n!} \cong 1 - \mu L \quad (8)$$

Therefore, detector response at 0° can be approximated as:

$$R \cong \varphi_0 \mu L \quad (9)$$

The response at 90° must account for the differences in chord lengths across the detector. The neutrons encounter different chord lengths across the detector ranging from 0 to diameter D, depending on the point of entry into the detector. The detector response can then be expressed as an integral over all chord lengths x_c:

$$R = \frac{2}{D} \int_0^{D/2} \varphi_0(1 - e^{-\mu x_c})dx \quad (10)$$

As Figure 8 shows, the Pythagorean theorem gives an expression for chord length x_c for each point along the vertical axis x, along which the incoming neutrons will be evenly distributed.

$$x_c = 2\sqrt{\left(\frac{D}{2}\right)^2 - x^2} \quad (11)$$

First, we substitute equation 11 into equation 10.

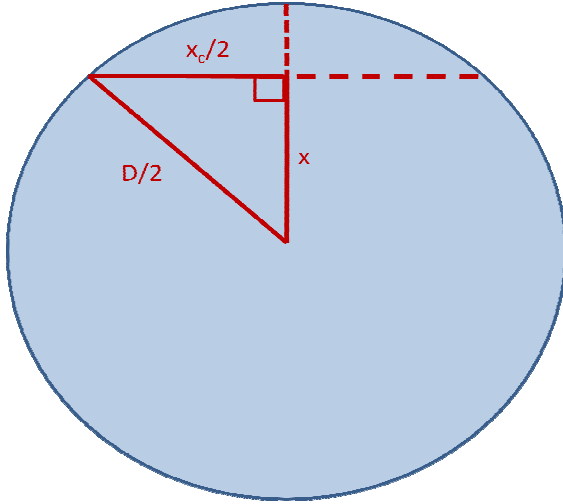$$R = \frac{2}{D} \int_0^{D/2} \varphi_0(1 - e^{-2\mu\sqrt{\left(\frac{D}{2}\right)^2 - x^2}})dx \quad (12)$$

Figure 8: Geometry of 90° neutron path across detector

Equation 12 does not lend itself to an analytical answer. Therefore, it is assumed that the path of each neutron will be approximately the mean chord length of a circle across the cylinder. It is unnecessary to consider the chord length across the cylinder itself because the analysis looks only to the first collision of the neutron, and all neutrons enter perpendicular to the cylindrical axis. The mean chord length of a circle is:

$$\bar{C} = \frac{\pi D}{4} \quad (13)$$

Using this information, we can apply equation 9 (the result for 0° neutrons) to the 90° neutrons, substituting the mean chord length for L as the distance uncollided neutrons traverse. This approximation yields:

$$R \cong \frac{\varphi_0 \mu \pi D}{4} \quad (14)$$

Taking a ratio of the two results and noting that the response functions have been normalized for incident flux, the ratio of the response functions will be:

$$\frac{R(\frac{\pi}{2})}{R(0)} \cong \frac{\frac{\varphi_0 \mu \pi D}{4}}{\varphi_0 \mu L} = \frac{\pi D}{4L} \quad (15)$$

The height of the detector in this problem is equal to the diameter, so:

$$\frac{R(\frac{\pi}{2})}{R(0)} \cong \frac{\pi D}{4D} = \frac{\pi}{4} \cong 0.79 \quad (16)$$

Therefore, the ratio of the 90° response to the 0° response is expected to be 0.79, which is approximately 25% higher than the 0.59 ratio that was calculated from the simulation. This result is reasonably congruent with the predicted value given the number of approximations that were made to reach it.

Obtaining the expected result for the bare detector vindicates the efficacy of this simulation. Because there is no moderating material, this simple case should reflect the geometry of the simulation's setup. The results of the simulation suggest that the difference in geometry is the driving force behind the differences in detector response, which lends credence to this method of analysis.

Although this cursory analysis verifies the efficacy of the techniques used in this experiment for calculating Bonner Sphere response, there are additional considerations that could undermine this result in other applications. First, the macroscopic cross section in the MCNPX neutron libraries varies as a function of energy, a fact that has been neglected in this analysis. Second, Figure 7 shows that the ratio of response function appears to increase at very low energies. Although this research did not merit an additional examination of this characteristic, it is likely that the increased response is due to the low penetrating powers of low-speed neutrons. The low-energy neutrons are less likely to pass uncollided through the detector, so the Taylor

approximation utilized to obtain the ratio may not be as accurate as it is for higher energy neutrons.

Impact of Moderating Material on Response

The straightforward geometric relationship derived for the difference of the detector response function between 0 and 90° does not translate to an easily analyzed relationship for detectors surrounded by moderating material. Figures 9 through 14 show the 0 and 90° simulation results for all Bonner Spheres.
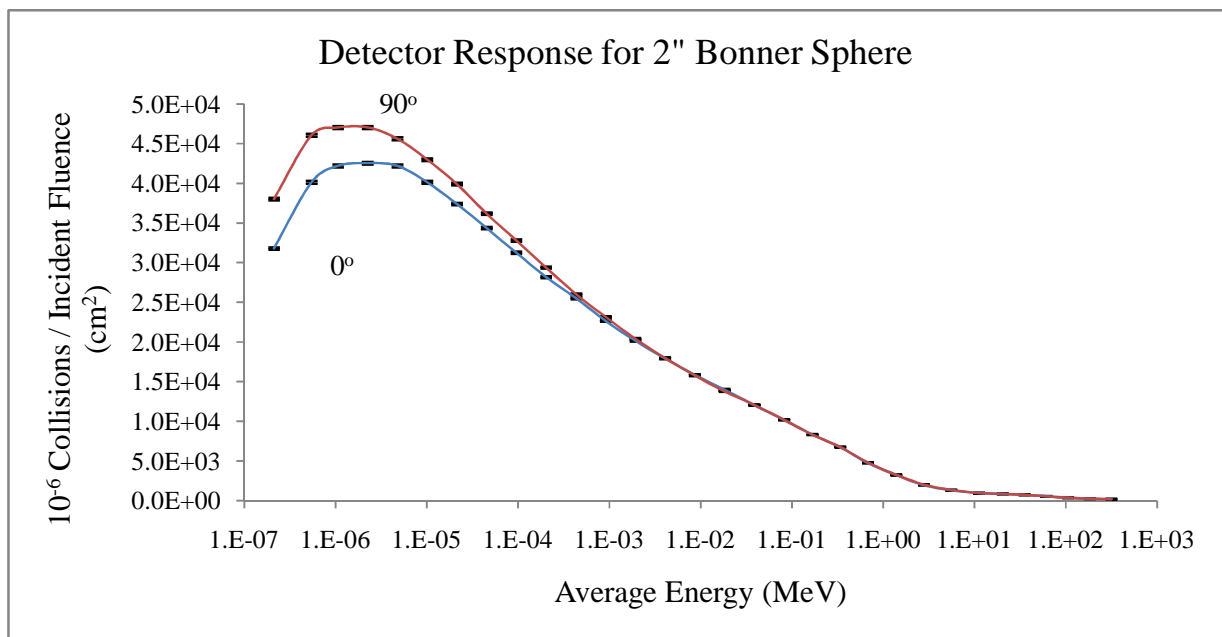

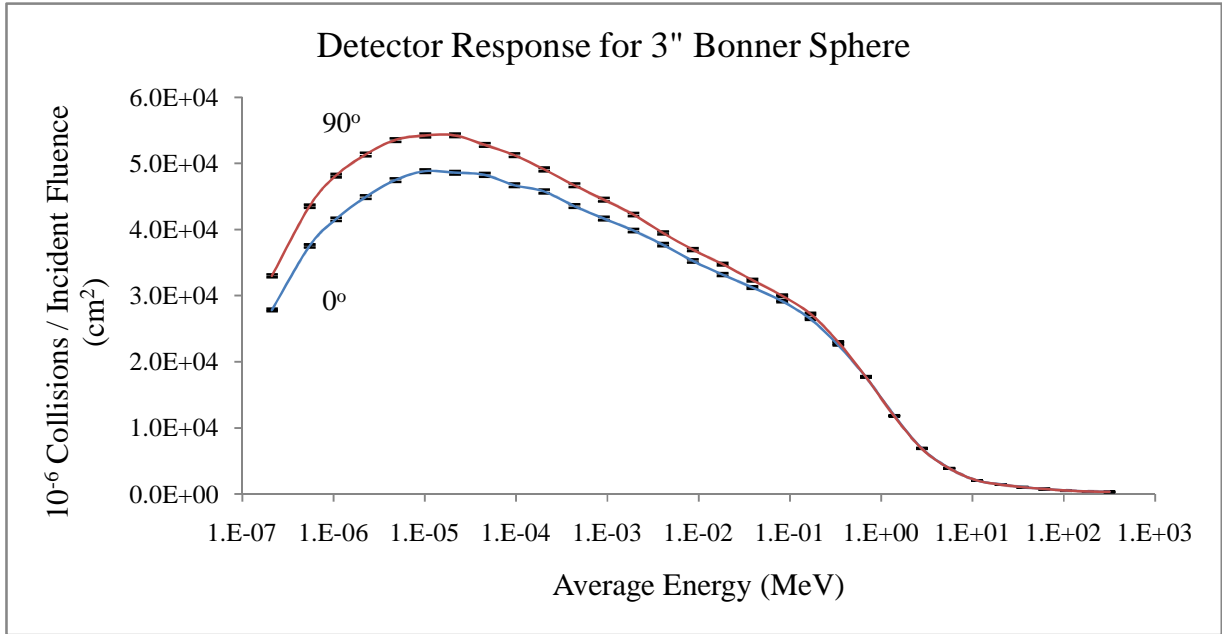
Figure 9: Detector Response for 2" Bonner Sphere
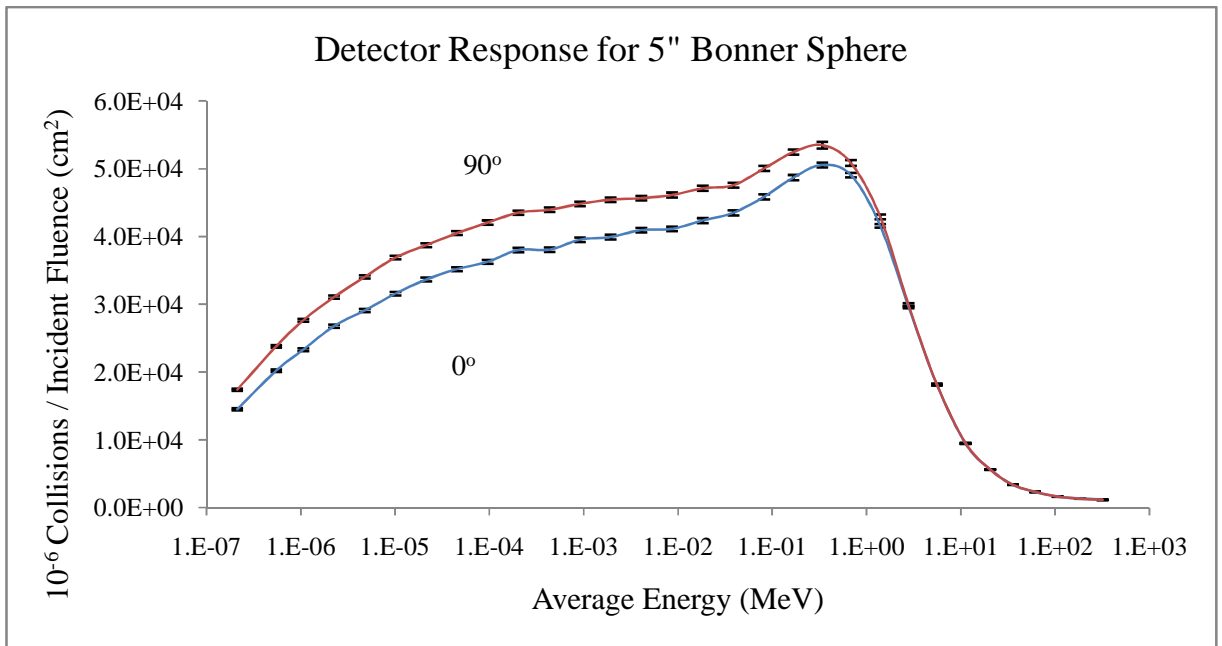
Figure 10: Detector Response for 3" Bonner Sphere

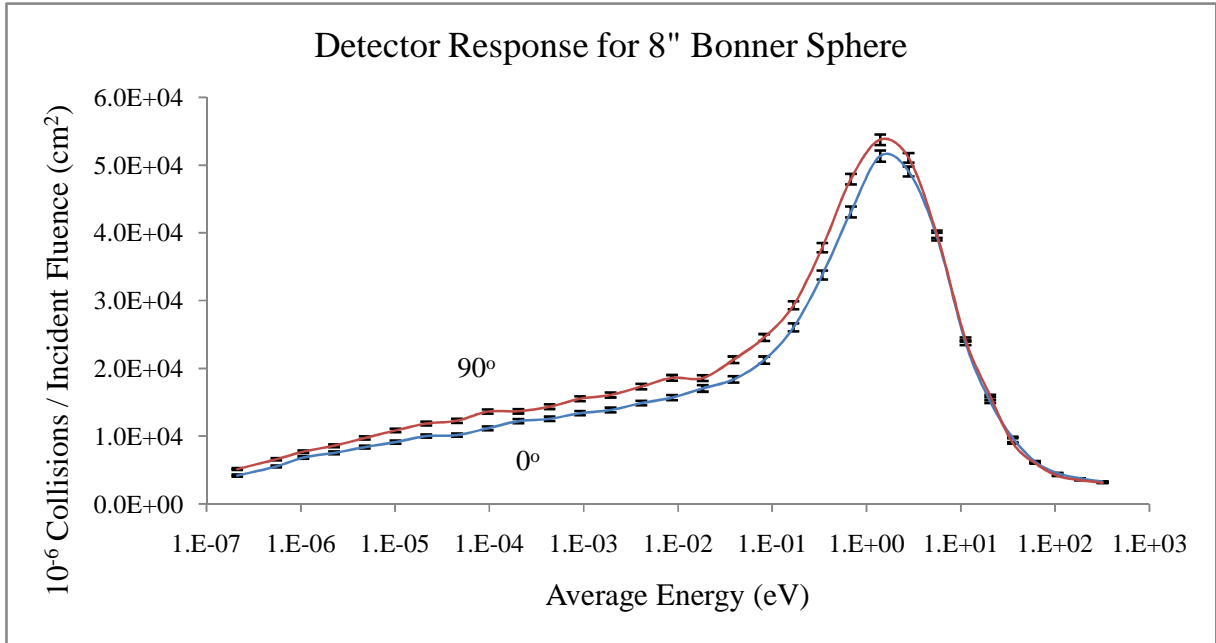**Figure 11: Detector Response for 5" Bonner Sphere**

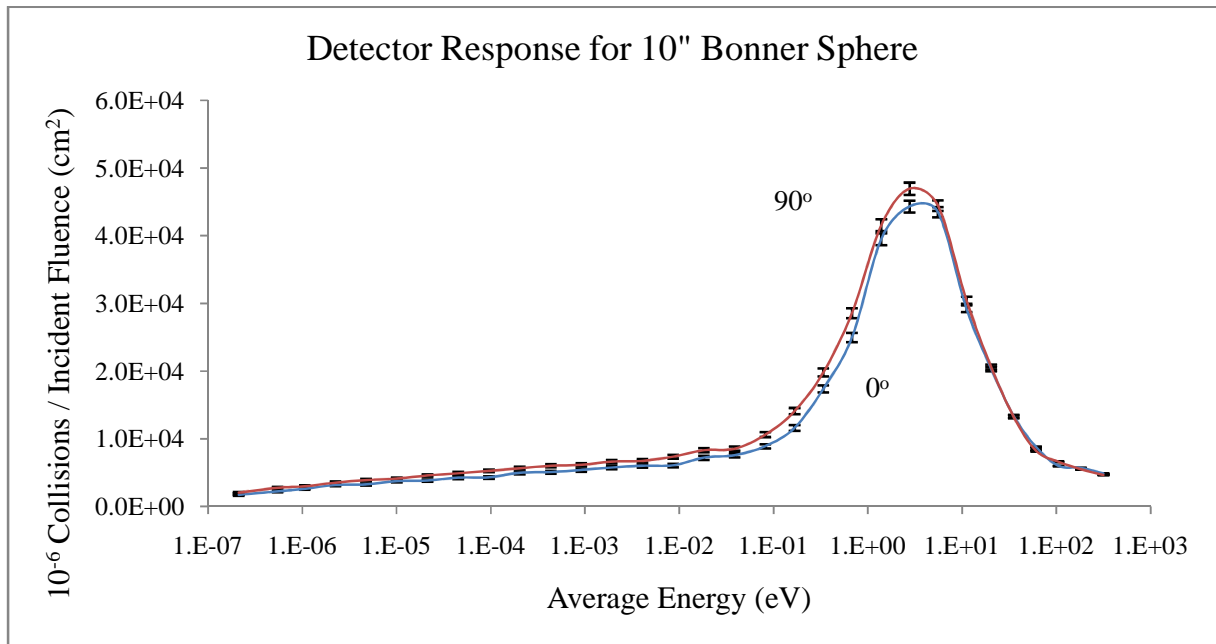**Figure 12: Detector Response for 8" Bonner Sphere**

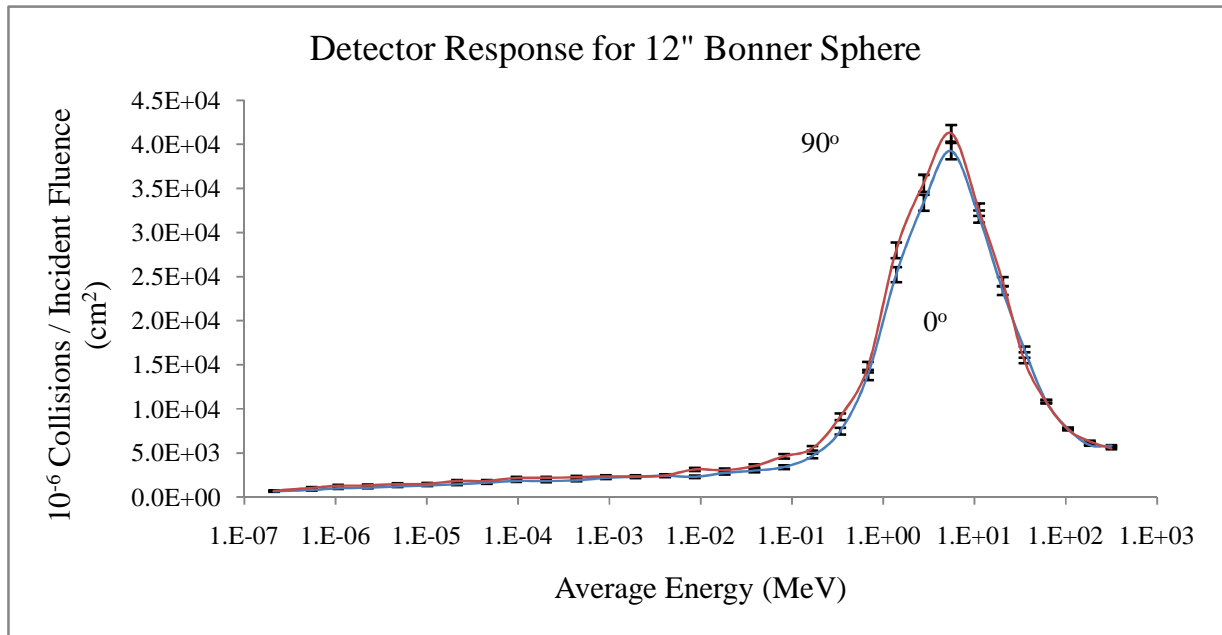**Figure 13: Detector Response for 10" Bonner Sphere**

Figure 14: Detector Response for 12" Bonner Sphere

At least two important differences come into play when the detector is surrounded by a Bonner Sphere. First, it is no longer reasonable to calculate the detector response analytically by assuming that only once-collided neutrons will contribute to the detector response. Indeed, the theory behind Bonner Spheres relies on their moderating effects through multiple collisions to produce varied responses among the different-sized spheres. As a result, most of the neutrons entering a detector inside a Bonner Sphere will have scattered from the moderating material at least once. Because of their multiple scattering collisions, it is expected that the flux incident on the detector inside a Bonner Sphere will be much closer to isotropic than the decidedly non-isotropic flux incident on the spheres in this simulation. A large amount of scattering inside the Bonner Sphere will result in the flux becoming asymptotically more isotropic. As the flux becomes more isotropic, it is expected that the response function's dependence on borehole orientation should diminish.

A qualitative assessment of the number of scattering collisions that a given neutron will undergo prior to entering the detector gives a rough estimate of how close to the isotropic limit the detector response is expected to be. On one hand, it is unlikely that neutrons born at low-energy colliding in the detector have undergone many scattering collisions prior to entering the detector. Those neutrons that do scatter become less and less likely to reach the detector because they become more likely to be absorbed in the polyethylene sphere, so it follows that the flux for low-energy neutrons is likely to maintain the anisotropic character of the incident flux. On the other hand, high-energy neutrons are likely to undergo many scattering collisions prior to entering the detector. As the high-energy neutrons scatter and lose energy, their angular flux will more closely approximate an isotropic flux. Because the neutrons born at higher energies undergo a greater number of collisions prior to interacting in the detector, there is a higher chance that a neutron interacting in the detector has undergone a backscatter collision.

Figure 15 confirms this qualitative assessment: it shows that for each sphere, the ratio of response functions varies from a value of about 1.2 for the lowest energy bins to approximately 1 for the highest energy bins. These response function ratios indicate the anisotropy of the surviving neutrons that are incident on the detector. High energy neutrons require many scattering collisions to moderate to the low energies to which the detector is most sensitive and are therefore more likely to approximate an isotropic flux. Low energy neutrons require few collisions to moderate to the energies to which the detector is sensitive. Many of the low-energy neutrons reaching the detector may be uncollided, which leads to a much more anisotropic flux at lower initial energies.

The higher variance in the larger diameter spheres makes the establishment of a statistical relationship between the differences for the smaller and larger spheres difficult. The

establishment of this relationship is left for further research in this area. Figure 16 depicts the

same graph but displays only the smaller spheres for visualization.
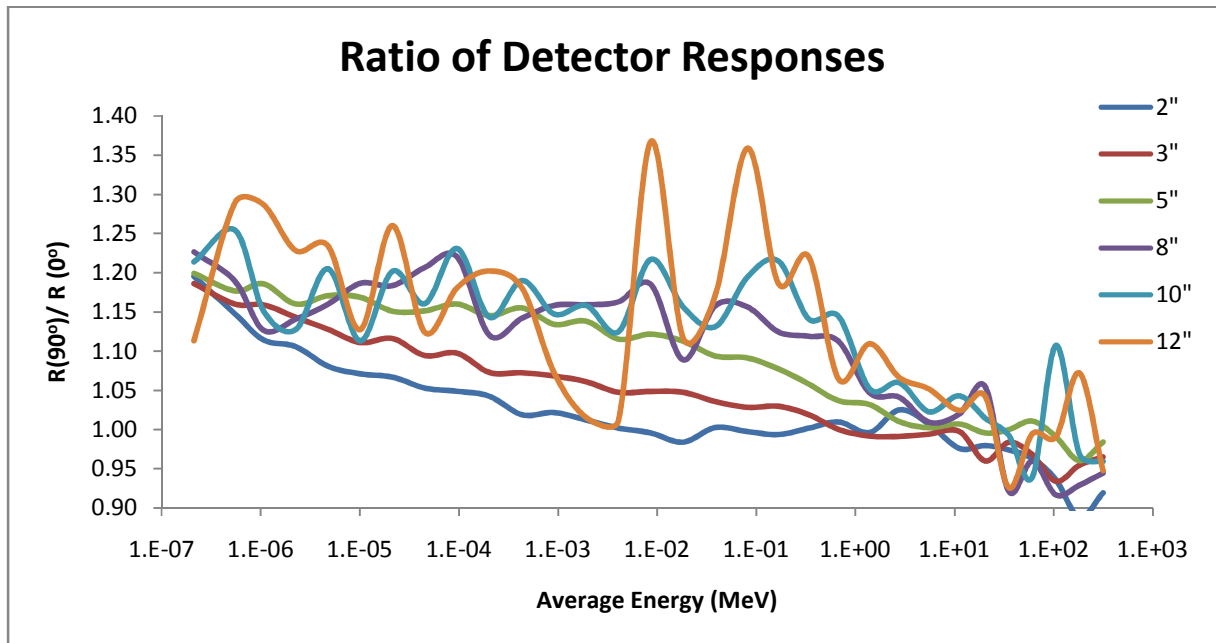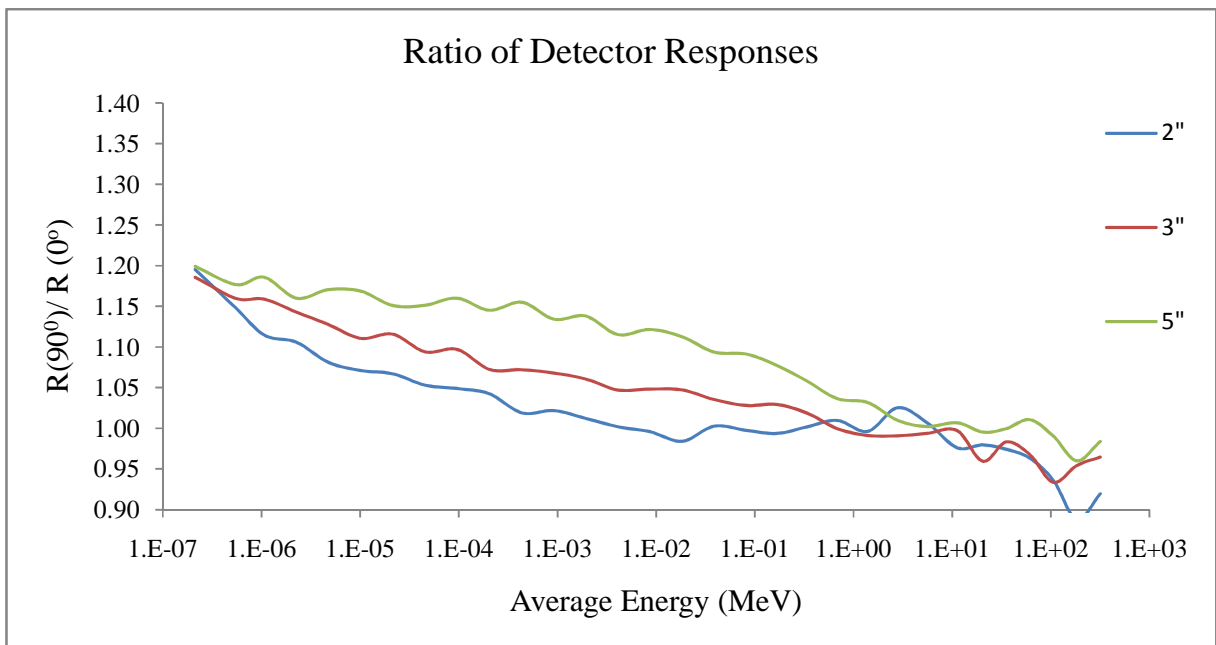

Figure 15: Ratio of Detector Responses

Figure 16: Ratio of Detector Responses for 2", 3", and 5" Bonner Spheres

A closer examination of Figure 15 and 16 reveals that for each sphere, the response function ratio is approximately the same at the highest and lowest energy bins. For the intermediate energy bins, the response function ratio of the smaller spheres approaches 1 faster than it does for the larger spheres. This result may seem counterintuitive because it would seem logical that the larger spheres would be more able to produce a near-isotropic flux inside the detector regardless of the incident energy. The point at which the response drops to near unity correlates with the response function tapering to zero at higher energies, which occurs earlier for smaller spheres. In essence, the flux at the center of the Bonner Sphere at this point is as isotropic as it will get. Therefore, the response function ratio's convergence on unity at higher energy is most likely due to two effects—the increased number of scattering events required to scatter the neutrons into the detector and the decrease of the response function due to the higher penetrating power of higher energy neutrons.

Effects of Bonner Sphere Geometry

One notable difference between the bare detector simulation results and the moderated response is the marked change in the 90° / 0° detector response function ratio when moderating material is added. For the bare detector, the results nearly matched the expected geometric result: the detector oriented at 0° responded significantly more than the detector oriented at 90°. When the detector was surrounded with a Bonner Sphere, the opposite was true: the detector oriented at 90° was more responsive, especially at lower energies. This simulation result suggests that the detector geometry does not have a significant effect on the response function when the detector is surrounded by moderating material.

Figure 17 highlights two potential sources of this effect. First, the borehole containing the detector is not filled with moderating material. The simulation included a glass rod which

held the detector in place, but the glass rod was not as effective at moderating neutrons as the polyethylene in the Bonner Sphere. The location of the borehole and its lack of moderating power can clearly have some impact on the detector response. Second, the Bonner Sphere geometry involves a borehole that is drilled only to the center. The edge of the detector touches the center, but the body of the detector is off-center. Therefore, when the apparatus is rotated 90°, the detector is physically closer to the source, and there is less moderating material between the detector and the source.

Three different simulations were run using the 2" sphere in an effort to ascertain the source of this difference. Figure 18 shows the response function ratios for the four different scenarios. Figure 18 only shows the ratio up to 1 MeV because of the high variance of this simulation at the higher energies. The first simulation shows the original detector geometry, which is also displayed in Figures 15 and 16.
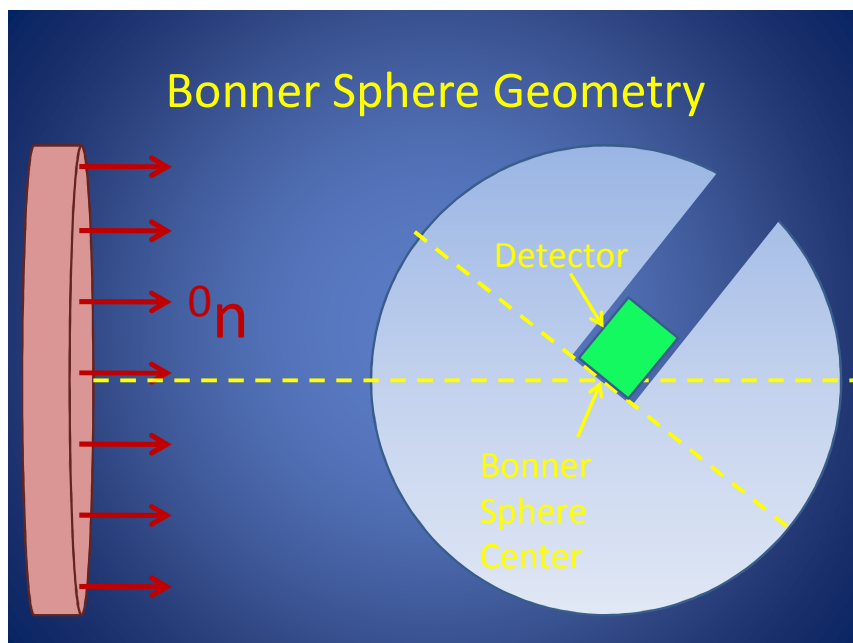

Figure 17: Simulation Setup, illustrating the geometric center of the Bonner Sphere
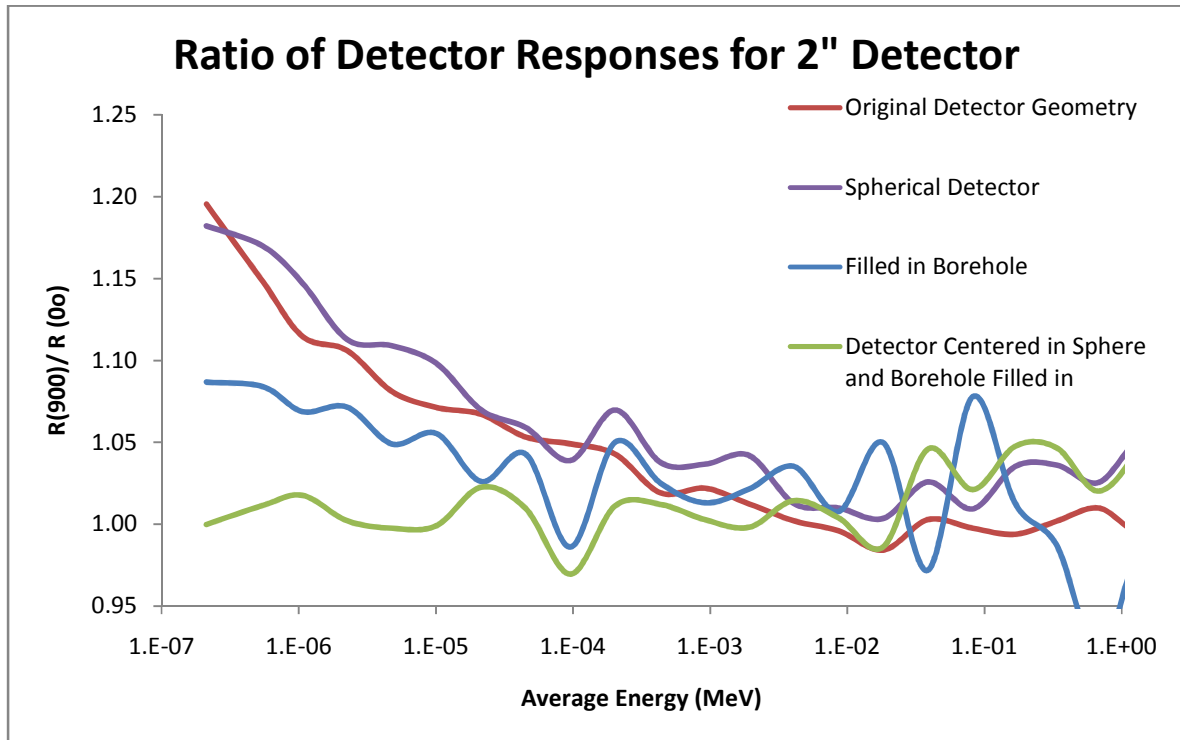
Figure 18: Response Function Ratios for various hypothetical scenarios

The second simulation replaced the detector with a spherical detector of the same volume. This simulation should illustrate the effect that the detector orientation has on the simulation. Figure 18 shows that replacing the cylindrical detector with a spherical detector made no significant different to the response function ratio.

The third simulation used the original detector geometry, but the borehole was entirely filled in with polyethylene. This scenario isolated the effect of the borehole on the response function. Figure 18 shows that this geometry reduces the detector response ratio from approximately 1.2 at the lowest energies to approximately 1.1, illustrating that the borehole is at least partially responsible for the difference in detector response function.

The fourth simulation includes a filled in borehole and places the detector at the geometric center of the sphere rather than at the edge of the borehole. As Figure 18 indicates, filling in the borehole with polyethylene and translating the detector to the center of the sphere

virtually eliminates the difference in detector response function. The detector response function is virtually flat at one.

These calculations tend to show three things. First, they show that the response function does not depend on the geometry of the detector when the detector is surrounded by moderating material. Second, they show that the absence of moderating material in the borehole is at least partially responsible for the differences between the response function at 0 and 90$^\text{o}$. Third, they show that the offset of the detector from the geometric center of the sphere is also responsible in part for the difference in detector responses. Although a full verification of these effects is left for further research, it appears that the absence of moderating material in the borehole and the offset of the detector from the center of the Bonner Sphere account for all of the differences in the detector response function between the 0- and 90$^\text{o}$-rotated Bonner Spheres in an anisotropic neutron field.

Conclusion

These results illustrate that Bonner Sphere detector response varies based on the direction of the incident neutron field. Furthermore, the results show that this difference is a function of the incident neutron energy, which could introduce significant error if an unfolding code that assumes an isotropic flux is applied in an anisotropic neutron field. With additional research, a well-defined response function ratio to energy relationship could be produced, which could then be incorporated into future unfolding codes to account for unidirectional flux. Additional research should also examine the effects of other anisotropic flux scenarios such as a bidirectional flux to determine if the relationships determined in these simulations can be applied directly or used to calculate a measure of anisotropy that could be calculated for different source problems and included in unfolding codes.

References

R.L. Bramblett, R.I. Ewing, & T.W. Bonner, *A New Type of Neutron Spectrometer*, 9 Nuclear Instruments and Methods 1-12 (1960).

J.A. Cruzate, J.L. Carelli, & B.N. Gregory, Bonner Sphere Spectrometer, presented at Workshop on Uncertainty Assessment in Computational Dosimetry: A Comparison of Approaches, Bologna, Italy (8-10 October 2007).

Glenn F. Knoll, Radiation Detection and Measurement (3rd ed), John Wiley & Sons, Inc. (2000).

D.B. Pelowitz, ed., *MCNPX User's Manual* (Feb. 2008 ed.).

Jeremy Sweezy, Nolan Hertel, & Ken Veinot. BUMS—Bonner Sphere Unfolding Made Simple: an HTML based multisphere neutron spectrometer unfolding package. 476 Nuclear Instruments and Methods in Physics Research A 263-69 (2002).

X-5 Monte Carlo Team, *MCNP--A General Monte Carlo N-particleTransport Code, Version 5* (Feb. 2008 ed.).

Vita

John Brittingham was born in Nashville, Tennessee and grew up both there and in Atlanta, Georgia. After graduating from high school, he attended Yale University, where he majored in physics. John then served as a submarine officer in the United States Navy, completing his active duty service in Millington, Tennessee. During his last few months in the Navy, John began work on the Master of Science in Nuclear Engineering through the University of Tennessee's distance education program. John completed the program in December 2010.